Author Manuscript

Author Manuscript

Author Manuscript

Author Manuscript

HHS Public Access

Author manuscript

J Invest Dermatol. Author manuscript; available in PMC 2013 November 01.

Published in final edited form as:

J Invest Dermatol. 2013 May ; 133(5): 1311–1320. doi:10.1038/jid.2012.419.

Ptch1 overexpression drives skin carcinogenesis and developmental defects in *K14Ptch*^{FVB} mice

Hio Chung Kang[1], **Yuichi Wakabayashi**[2], **Kuang-Yu Jen**[3], **Jian-Hua Mao**[4], **Vassilis Zoumpourlis**[5], **Reyno Del Rosario**[1], and **Allan Balmain**[1]

[1]Comprehensive Cancer Center, University of California, San Francisco, San Francisco, CA, USA

[2]Division of Experimental Animal Research, Chiba Cancer Center Research Institute, Nitonamachi Chuouku Chiba-city, Chiba-prefecture, Japan

[3]Department of Pathology, University of California, San Francisco, San Francisco, CA, USA

[4]Life Sciences Division, Lawrence Berkeley National Laboratory, One Cyclotron Road, Berkeley, CA, USA

[5]National Hellenic Research Foundation, Institute of Biology, Medicinal Chemistry & Biotechnology, Athens, Greece

Abstract

Ptch1 is a key regulator of embryonic development, acting through the sonic hedgehog (SHH) signaling pathway. Ptch1 is best known as a tumor suppressor, since germline or somatic mutations in *Ptch1* lead to the formation of skin basal cell carcinomas (BCCs). Here, we show that *Ptch1* also acts as a lineage-dependent oncogene, as overexpression of *Ptch1* in adult skin in *K14Ptch*^{FVB} transgenic mice synergizes with chemically induced *Hras* mutations to promote squamous carcinoma development. These effects were not due to aberrant activation of SHH signaling by the *K14Ptch*^{FVB} transgene, as developmental defects in the highest expressing transgenic lines were consistent with inhibition of this pathway. Carcinomas from *K14Ptch*^{FVB} transgenic mice had only a small number of non-proliferative *Ptch1* transgene positive cells, suggesting that the *Ptch1* transgene is not required for tumor maintenance, but may play a critical role in cell fate determination at the initiation stage.

Introduction

Ptch1 is a key signaling receptor in the sonic hedgehog (SHH) signaling pathway, which is critical in embryonic development, tissue patterning, and cell fate decisions (Chen, 1996; Ingham, 1991; Marigo *et al*., 1996). Mutations resulting in loss of Ptch1 function or aberrant expression of genes in the SHH pathway lead to developmental defects and a cancer-prone

Users may view, print, copy, and download text and data-mine the content in such documents, for the purposes of academic research, subject always to the full Conditions of use:http://www.nature.com/authors/editorial_policies/license.html#terms

Correspondence: Allan Balmain, Helen Diller Family Comprehensive Cancer Center, University of California San Francisco, San Francisco, CA 94158, USA. abalmain@cc.ucsf.edu.

Conflict of Interest

The authors state no conflict of interest.

Author Manuscript Author Manuscript Author Manuscript Author Manuscript

phenotype. Germline mutations in the human *PTCH1* gene are responsible for Gorlin syndrome (also called nevoid basal cell carcinoma syndrome, NBCCS), which is characterized by various developmental malformations and a high predisposition to skin basal cell carcinoma (BCC) development (Hahn, 1996; Johnson *et al*., 1996). Mice partially deficient in functional Ptch1 exhibit developmental abnormalities that are comparable to those of NBCCS patients. Additionally, these mice develop tumors such as medulloblastomas, rhabdomyosarcomas, and BCCs following ultraviolet (UV) or ionizing radiation exposure, demonstrating a critical role for Ptch1 in the regulation of developmental homeostasis and tumor suppression (Aszterbaum, 1999; Goodrich, 1997; Hahn *et al*., 1998).

We have previously identified a polymorphic variant in the mouse *Ptch1* gene ($Ptch^{FVB}$) that conferred susceptibility to early post-natal squamous cell carcinoma (SCC) development in transgenic mice expressing a mutant *H-ras* gene under the control of the keratin 5 promoter (*K5Hras* mice) (Wakabayashi *et al*., 2007). In this model, both Ptch1 and activated Ras are expressed under the control of constitutive keratin promoters during skin development (Byrne *et al*., 1994), and it remained possible that this paradoxical effect of Ptch1 in promoting cancer may be linked to developmental abnormalities related to this specific model. Therefore, we tested the role of Ptch1 in adult-onset skin tumor formation using the classical DMBA(dimethylbenzanthracene)/TPA(12-*O*-tetradecanoylphorbol-13-acetate) model involving sporadic mutation of the endogenous *H-ras* gene, rather than the high levels of mutant *H-ras* expressed during development in the *K5Hras* transgenic mice. Our data demonstrate that even low levels of *Ptch1* transgene expression that do not perturb expression of Gli transcription factors promote formation of malignant SCCs. We conclude that the SHH pathway can play either positive or negative roles in development of alternative tumor types within the same tissue.

Results

Developmental abnormalities in K14Ptch^{FVB} mice are consistent with diminished Hedgehog signaling

We previously generated four different transgenic lines (lines 6, 7, 8, and 10) expressing $Ptch^{FVB}$ under the control of the *K14* promoter at variable levels, with line 6 showing the highest *Ptch1* transgene expression (Wakabayashi *et al*., 2007). Initially, these transgenic lines were generated and maintained on the FVB/N background. Continuous breeding to the same background resulted in poor litter sizes, particularly in line 6 with the highest $Ptch^{FVB}$ levels. To maintain this line, we crossed the line 6 $K14Ptch^{FVB}$ mice to wild-type C57BL/6 mice and obtained litters on this hybrid background. We observed major phenotypic abnormalities in the line 6 $K14Ptch^{FVB}$ mice on both FVB/N and hybrid backgrounds. First, when compared to their wild-type littermates, line 6 $K14Ptch^{FVB}$ mice exhibited shorter mean body lengths (5.6 ± 0.48 cm vs. 7.9 ± 0.25 cm, P=0.00065 by t-test) and lower mean body weights (5.9 ± 0.74 g vs. 14.7 ± 0.68 g, P<0.00001 by t-test) at 4 weeks of age (Figure 1a). This smaller body size was not visible in the other transgenic lines apart from a slight size difference in line 8 $K14Ptch^{FVB}$ mice (data not shown). Furthermore, while the wild-type littermates showed normal eye development, line 6 $K14Ptch^{FVB}$ mice clearly displayed ocular defects involving bilateral and unilateral underdevelopment of the ocular structures

Author Manuscript Author Manuscript Author Manuscript Author Manuscript

(Figure 1b). Newborn line 6 *K14Ptch*^{FVB} mice exhibited either aphakia with microphthalmia (Figure 1b, upper middle panel), or anophthalmia (Figure 1b, upper right panel). Similar ocular defects have been described in mice with mutations in Gas1, a membrane-bound glycoprotein that is known to antagonize SHH signaling (Lee *et al*., 2001a, 2001b; Seppala *et al*., 2007). Adult line 6 *K14Ptch*^{FVB} mice demonstrated complete and permanent closure of the developmentally abnormal eyes (Figure 1b, lower panel). Finally, just as limb deformities have been linked to defects in both mouse and human genes involved in the SHH pathway, the line 6 *K14Ptch*^{FVB} mice displayed abnormal limb development (Figure 1c). Both forelimbs and hindlimbs of line 6 *K14Ptch*^{FVB} mice showed oligodactyly with fewer digits, consistent with a general inhibition of SHH signaling during mouse development. The defective eyes and limb deformities were not observed in lines 7 and 8 *K14Ptch*^{FVB} mice. These phenotypic abnormalities in *Ptch1* transgenic mice are clearly opposite to those observed in *Ptch1*$^{+/-}$ mice or animals expressing transgenic *Shh* (Goodrich, 1997; Oro *et al*., 1997). We conclude that the *Ptch1* transgene, although expressed in a subset of tissues under the control of the *K14* promoter, is acting in the expected fashion as an inhibitor of SHH signaling during mouse development.

K14Ptch^{FVB} mice develop a higher frequency of chemically induced skin carcinomas than wild-type mice

To explore the oncogenic function for *Ptch1* in the setting of adult onset skin carcinoma development, we performed two-stage skin carcinogenesis by treating DMBA followed by TPA. Because of the difficulties in breeding the line 6 transgenic mice, we carried out the carcinogenesis studies with lines 7 and 8 transgenic mice on the FVBxC57BL/6 F1 genetic background (Wakabayashi *et al.*, 2007). By 20 weeks post-treatment, both lines of *K14Ptch*^{FVB} transgenic mice and wild-type mice developed a similar number of papillomas, (Figure 2a, P=0.89 by Kruskal-Wallis test). It is known that a subset of benign papillomas induced by DMBA/TPA progress to malignant squamous (SCCs), or spindle cell carcinomas (SpCCs) (Burns, 1991; Oft *et al*., 2002). Thus, we monitored the mice for carcinoma development for up to 50 weeks post-TPA treatment. At this time point, 71% of line 7 *K14Ptch*^{FVB} mice and 84% of line 8 *K14Ptch*^{FVB} mice had developed carcinomas, compared to only 35% of wild-type mice (Figure 2b) (P=0.023 for line 7, P=0.0011 for line 8 by Fisher's exact test). The carcinoma latency period was significantly shortened in *K14Ptch*^{FVB} mice compared to wild-type mice, which translated to lower carcinoma-free survival at 50 weeks (Figure 2c, P=0.0027 by Kaplan-Meier method). The skin carcinomas were either SCCs or SpCCs in both *K14Ptch*^{FVB} and wild-type mice, with no difference in terms of the frequency of histological subtypes (Table S1). A hallmark of DMBA-initiated skin tumors is activating *H-ras* mutations at codon 61(CAA to CTA, Gln to Leu) (Balmain, 1984; Quintanilla *et al*., 1986). A similar codon 61 CTA mutation frequencies was detected in carcinomas from *K14Ptch*^{FVB} (24/27; 89%) and wild-type (10/11; 91%) mice (Table S1). Taken together, these data support a positive role of Ptch1 expression in promoting sensitivity to carcinoma development initiated by mutation of Ras in adult mice.

Effect of oncogenic H-Ras and TPA treatment on Ptch1 binding to Tid1

We previously showed that the product of the mouse *Tid1* tumor suppressor gene showed differential binding to Ptch^{FVB} and Ptch^{B6} in 293T cells (Wakabayashi *et al.*, 2007). In

Author Manuscript Author Manuscript Author Manuscript Author Manuscript

order to explore the possible mechanisms by which *Ptch1* expression may interact with H-Ras signaling, we investigated the effects of *H-RAS* transfection or TPA treatment on, Tid1-Ptch1 binding and on activation of the MapK signaling pathway. Figure 3a shows that transfection of mutant *HRAS* into 293T cells led to accumulation of the GTP-bound form of RAS, but surprisingly had only a minor effect on activation of phospho-Erk (P-Erk) (Figure 3a, lanes 1–2). Co-transfection of *Ptch1* ($Ptch^{FVB}$ or $Ptch^{B6}$) in this assay led to only a modest but reproducible stimulation of P-Erk, and this was increased slightly by co-transfection of oncogenic V12*HRAS.* In parallel experiments, oncogenic *HRAS* had little influence on the binding of Tid1 to $Ptch^{FVB}$ or $Ptch^{B6}$ as shown by co-immunoprecipitation assays (Figure 3b). However, TPA treatment that had a very strong effect on the activation of P-Erk (Figure 3c, second to bottom panels) destabilized the strong binding between Tid1 and Ptch1, especially for the $Ptch^{B6}$ variant (Figure 3c, lanes 3 and 4). This reduced level of binding, seen both at 30 min and 1hr after TPA treatment, was more similar to that seen with the FVB variant protein, suggesting that activation of HRAS/Mapk signaling may directly affect the stability of the Ptch1-Tid1 complex.

Gene expression analysis of SHH signaling targets in *K14Ptch^{FVB}* mouse skin and skin carcinomas

Loss of the inhibitory function of Ptch1 in the SHH signaling pathway results in up-regulation of *Gli1*, *Gli2*, and *Ptch1* itself (Aszterbaum, 1999; Dahmane *et al*., 1997). To investigate whether *Ptch1* overexpression in skin and skin SCCs gives rise to perturbations in SHH signaling, we performed qRT-PCR for the major target genes *Ptch1*, *Gli1*, *Gli2*, as well as *Ccnb1* (*cyclin B1*) which was proposed to act together with *Ptch1* in regulating the cell cycle (Barnes *et al*., 2001). While the average transcript level of total *Ptch1* was elevated in skin (Figure 4a, $P<0.0001$ by t-test), and to a lesser extent also in skin cancers from *K14Ptch^{FVB}* mice (Figure 4b, $P=0.0014$ by t-test), *Gli1* and *Gli2* levels in skin (Figure 4a) and skin carcinomas (Figure 4b) were comparable between *K14Ptch^{FVB}* and wild-type mice. The average *Ccnb1* transcript level was not different between the two genotypes, both in normal skin and in skin tumors (Figure 4a–b). We conclude that all of these known SHH pathway candidate genes are not significantly disrupted in expression levels, at least at the whole tissue level, in *Ptch1* transgenic skins.

To investigate other possible consequences of *Ptch1* overexpression in *K14Ptch^{FVB}* mice, we chose candidate genes on the basis of correlation in transcript levels with *Ptch1* in normal skin from interspecific backcross mice (Quigley *et al*., 2009; additional data not shown). We performed qRT-PCR analysis for eight candidate genes – *Bmp6*, *Bnc2*, *Hdgfrp3*, *Nt5e*, *Sox4*, *Gli3*, *Lphn1*, *Ncdn*, all of which were significantly correlated with *Ptch1* expression in normal skin. The expression analysis showed that only the *Sox4* transcript level was significantly decreased in adult skins of *K14Ptch^{FVB}* mice compared to controls (Figure 4c, $P=0.001$ by t-test), but no difference was seen in skin carcinomas (Figure 4b). This reduced level of *Sox4* was also seen, but to a lesser extent in, newborn skins from lines 6 and 8 *K14Ptch^{FVB}* mice (Figure 4d, $P=0.023$ by t-test).

Author Manuscript Author Manuscript Author Manuscript Author Manuscript

Presence of Ptch1 transgene positive cells in skin carcinomas

To examine *Ptch1* transgene expression at the cellular level in skin and skin carcinomas from transgenic mice, we carried out an immunohistochemical analysis using antibodies against the HA tag present at the C-terminus of the Ptch1 transgene. Cells positive for anti-HA were simultaneously positive for anti-Ptch1 by co-staining. First, we evaluated normal skin from the *K14Ptch*^{FVB} transgenic lines for the presence of HA/Ptch-positive epithelial cells. Among the three *K14Ptch*^{FVB} transgenic lines, a small number of HA/Ptch positive cells was only detectable in skin from line 6 *K14Ptch*^{FVB} mice (Figure 5a). These HA/Ptch positive cells were clustered in small foci rather than being scattered as single cells at the basal layer of the epidermis (Figure 5a). On the other hand, no HA-positive cells were identified in skin from lines 7 and 8 *K14Ptch*^{FVB} mice. It appears that while the *Ptch1* mRNA level remains elevated in adult skin from *K14Ptch*^{FVB} mice compared to wild-type mice, significant protein expression is only detectable in clusters of epidermal cells during development.

Next we examined the presence of HA/Ptch positive cells in skin carcinomas from *K14Ptch*^{FVB} mice. Of 24 transgenic mouse carcinomas tested, 20 (83%) showed small clusters of HA/Ptch positive cells, but none were detected in carcinomas from wild-type mice (Table S1). These cells were mainly detected in SCCs, and if present in SpCCs, they were predominantly in areas of the tumor that showed squamous differentiation (Figure 5b–c). In the SCCs, the HA/Ptch positive cells were located at the superficial aspect of the spinous layer, near the interface with the keratinized/cornified cells (Figure 5b), particularly in tumor regions with strong keratin 14 expression (Figure 6a). The cell proliferation marker, Ki67, was frequently expressed in the skin cancer cells, but the HA/Ptch positive cells (78–100%) were largely negative for Ki67 expression (Figure 6b), indicating that these cells are likely non-proliferative. We also performed co-staining of the known skin stem cell markers, Sox2, Pax6, or Cd34, with the HA/Ptch tag (Takahashi, 2008; Li, 2005; Malanchi *et al*., 2008). Some HA/Ptch positive cells showed co-staining with Sox2 and Pax6, but the pattern was essentially random (Figure 6c), and these cells were largely negative for Cd34 (Figure 6c). We conclude that any HA/Ptch positive cells that are found in skin carcinomas are predominantly terminally differentiated cells with no significant proliferative and stem cell-like activity.

Discussion

In this study, we have explored the paradoxical role of exogenous *Ptch1* expression in promoting Ras-driven SCC development. Line 6 *K14Ptch*^{FVB} mice with the highest *Ptch1* overexpression had severe developmental defects including growth retardation, loss of digits in the fore- and hindlimbs, as well as abnormalities of the eyes. The similarity between these phenotypes and those caused by germline mutations leading to loss of SHH pathway function (Chiang, 1996; Chiang, 2001; Zhang *et al*., 2001) indicates that expression of Ptch1 driven by the K14 promoter during development (Byrne, 1994; Kopan *et al*., 1989) results in perturbation of Shh signaling by either cell autonomous or non cell-autonomous mechanisms, leading to the observed major developmental abnormalities in developing epithelia.

Author Manuscript Author Manuscript Author Manuscript Author Manuscript

Skin tumor susceptibility studies were performed on two transgenic lines (lines 7 and 8), in which *Ptch1* transgene expression was relatively low. Nevertheless, these lines were found to be highly susceptible to chemically induced carcinomas of the skin in a two-stage carcinogenesis study. Gene expression analysis detected no changes in the major downstream effectors of SHH signaling such as Gli1 or Gli2 in adult skin, although it remains possible that single cells or clusters of Ptch1-positive cells in transgenic skin could express altered levels of these markers. Of the other candidate genes selected based on correlations with *Ptch1* expression in heterogeneous mouse populations (Quigley et al, 2009), only *Sox4* was expressed at lower level in the skins of *K14Ptch*^{FVB} mice. A previous study suggested that *PTCH1* is one of the *SOX4* transcriptional target genes (Scharer *et al*., 2009), and coexpression of Sox4 and Shh in the developing hair germ was observed (Kobielak *et al*., 2007). It is therefore possible that one consequence of Ptch1 overexpression is deregulation of stem cell dynamics through a feedback leading to altered *Sox4* expression in *K14Ptch*^{FVB} mice. At the molecular level, *in vitro* studies using human 293T cells indicated that one possible mechanism by which Ptch1 and the Ras pathway interact is through modulation of Map kinase signaling. Strong activation of P-Erk by TPA led to disruption of the previously reported strong binding of the Ptch1 Ptch^{B6} variant to mTid1 (Wakabayashi et al, 2007), a tumor suppressor protein originally discovered in *Drosophila* (Canamasas *et al*., 2003). It is possible that activation of Ras/MapK signaling alleviates the tumor suppressor functions of Tid1 through reduction of its interaction with Ptch. Further studies using conditional knock-out alleles will be required to determine whether similar mechanisms play a role in promoting the growth of Ras-initiated cells in mouse skin.

We also tested the possibility that the subpopulation of cells within carcinomas that continued to express the Ptch1 transgene might be involved in tumor maintenance, or express markers of skin stem cells. However, these cells were only found in very well differentiated tumors, or in highly differentiated cells within more aggressive tumors. They were negative for expression of cell cycle marker, suggesting that they do not display proliferative activity, and were also negative for markers such as Cd34, Pax6 and Sox2 that have been implicated in control of skin stem cells. These data are compatible with the interpretation that the *Ptch1* transgene expression, although clearly acting to promote SCC development, is no longer required for the maintenance of these tumors and is silenced during tumor progression.

Our data are compatible with the hypothesis that the SHH pathway, when activated through loss of Ptch1 or activation of downstream effectors such as Smoothened (Smo) or Gli1/2, leads to increased susceptibility to BCC formation by promoting the cell fate decision leading to the appropriate cell of origin for these tumors. Overexpression of *Ptch1* however promotes an alternative epidermal cell fate decision leading to increased SCC formation. The concept that developmental regulators that promote one particular lineage can also simultaneously suppress an alternative lineage is well known (Davidson 2010). Such a mechanism may have an important influence on susceptibility to different types of tumors in the same tissue, conferring susceptibility to one type but resistance to an alternative tumor arising from a different lineage. Polymorphisms in genes that influence alternative cell fate

Author Manuscript Author Manuscript Author Manuscript Author Manuscript

decisions may therefore play an important role in determining individual tumor susceptibility at an early stage of carcinogenesis.

Materials and Methods

Mice, tumor induction, and histological analysis

All animal experiments were performed under the UCSF Institutional Animal Care And Use Committee (IACUC) approval. The original *K14Ptch*^{FVB} mice from lines 6, 7, and 8 were previously described (Wakabayashi *et al*., 2007). Lines 7 and 8 were maintained on the FVB/N background and crossed with C57BL/6 mice to generate F1 wild-type and K14Ptch^{FVB} mice for two stage chemical carcinogenesis. 23 line 7 *K14Ptch*^{FVB} and 26 line 8 *K14Ptch*^{FVB} mice along with 35 wild-type mice (combined from both lines) were used to induce chemical carcinogenesis. Mice were genotyped using PCR primers previously described (Wakabayashi *et al*., 2007). To induce skin carcinogenesis, a single dose of DMBA was topically applied at 8 weeks of age followed by twice-weekly application of TPA for 20 weeks as described (Balmain, 1984; Quintanilla *et al*., 1986). Papilloma number was recorded from 10 weeks post-DMBA up to 20 weeks and carcinoma development was monitored up to 50 weeks post-TPA treatment. Mice were sacrificed if they were moribund, if there were excessive tumor loads, if any single tumor exceeded 1.5 cm in diameter, or at the termination of the experiment. Tumors removed by surgical dissection were immediately snap-frozen in liquid nitrogen or fixed in 10% buffered formalin solution for further analysis. Paraffin-embedded tumor sections were stained with H&E for histopathological analyses.

DNA and RNA extraction

Frozen skin and tumor specimens were powdered in liquid nitrogen with pestle and mortar and homogenized for DNA and RNA preparation. For RNA extraction, specimens were homogenized and dissolved in TRIzol Reagent (Invitrogen, Carlsbad, CA) and purified for RNA isolation according to manufacturer's instruction. Genomic DNA was isolated using standard phenol/chloroform extraction following an overnight incubation at 55°C with Proteinase K (Sigma, St. Louis, MO) in a lysis buffer (50 mM Tris at pH 8.0, 100 mM EDTA, 100mM NaCl, 1% SDS).

H-ras mutation analysis

To determine a specific H-*ras* mutation, CAA to CTA at codon 61, exon 2 of the *H-ras* gene was amplified using the primers previously described (Nagase *et al*., 2003). Amplified PCR fragments was digested with restriction enzyme *XbaI* (NEB, Ipswich, MA) at 37°C for 2 hours and electrophoresed in a 4% Nusieve 3:1 agarose gel (Lonza, Walkersville, MD).

Cell culture and transfection

293T cells were grown at 37°C in DMEM supplemented with 10% FBS, penicillin, streptomycin, and glutamine and maintained in a humidified atmosphere of 5% CO_2. HA-tagged Ptch^{FVB} and Ptch^{B6} constructs in pcDNA3.1 and pLXSP3 retrovirus expressing V12*HRAS* were previously described (Wakabayashi et al., 2007). For transient transfection

Author Manuscript Author Manuscript Author Manuscript Author Manuscript

or co-transfection, Lipofectamine 2000 was used according to the manufacturer's instruction (Invitrogen, Carlsbad, CA)

Western blotting, immunoprecipitation, and Ras-GTP assays

Western blotting was performed as previously described (Wakabayashi et al., 2007). Antibodies ERK1/2 (137F5), P-ERK1/2 (20G11), Tid1 (RS13 and RS-11), H-Ras (C-20, sc-520), HA-tag (mouse monoclonal 6E2 and goat polyclonal ab9134), β-actin (from Sigma) were used. For TPA treatment, transfected 293T cells were incubated with 500nM of TPA for 30 min and 1 hour. For immunoprecipitation, 500ug of lysates were processed with HA Tag IP/Co-IP kit (Thermo Scientific, Waltham, MA) and Dynabeads Protein G IP kit (Invitrogen, Carlsbad, CA) according to manufacturers' instructions. For Ras-GTP assay, cells were washed with ice-cold PBS and lysed in 1X MLB (Magnesium-containing Lysis Buffer) with protease and phosphatase inhibitor cocktails. Raf-RBD pull down was performed with Ras Activation Assay kit containing Raf-1 RBD agarose beads according to manufacturer's manual (EMD Millipore, Billerica, MA).

Expression analysis for SHH signaling targets

Single strand cDNAs were synthesized from 1ug of DNase-treated total RNA from skins and skin carcinomas using SuperScript® III First-Strand Synthesis System (Invitrogen, Carlsbad, CA) according to manufacturer's manual. Pre-designed TaqMan probes and primers for Ptch1 (Mm01306905), Gli1 (Mm00494654), Gli2 (Mm01293111), Ccnb1 (Mm00838401), Sox4 (Mm00486317), Bmp6 (Mm01332882), Bnc2 (Mm01266537), Nt5e (Mm00501917), Hdgfrp3 (Mm01324333), Gli3 (Mm00492345), Lphn1 (Mm00492345), Ncdn (Mm00449529), Actb (beta-actin, 4352933E), and Gapdh (Mm99999915) were used for qRT-PCR analysis (ABI, Foster City, CA). Amplification of cDNAs was carried out in triplicate for each sample in the ABI 7900HT system according to the manufacturer's protocol. The normalized transcript level was determined by calculating dCt (delta Ct) values by subtracting mean Ct values of target genes with mean Ct values of housekeeping genes. Then, 1/dCt values were used to obtain representative values indicating higher values to higher transcript levels.

Immunofluorescence

Skin and carcinomas specimens were fixed in buffered formalin solution and processed for paraffin embedding. Sections (5μm in thickness) were de-paraffinized with xylene two times for 10 minutes and processed in a pressure cooker for antigen retrieval using Triology solution (Cell Marques, Rocklin, CA). The sections were blocked in 10% donkey serum supplemented with 0.3% Triton X-100 for 1 hour and incubated with primary antibody (HA tags, goat, Abcam, Cambridge, MA) for 1 hour at room temperature. After rinse with PBS, the sections were incubated with FITC-conjugated secondary antibody for 1 hour at room temperature. For double staining, HA tag incorporated sections were further blocked in 10% goat serum supplemented with 0.3% Triton X-100 for 1 hour and incubated with rabbit Ptch1 (Abcam, Cambridge, MA), Ki67 (Neomarkers, Fremont, CA), K14 (Covance, Princeton, NJ), Sox2 (Abcam, Cambridge, MA), Pax6 (Abcam, Cambridge, MA), or Cd34 (rat, BD Pharmingen, San Diego, CA) antibodies. After rinse with PBS, the sections were incubated with Alexa 555-conjugated anti-rabbit or anti-rat secondary antibodies followed

Author Manuscript Author Manuscript Author Manuscript Author Manuscript

by DAPI staining. The section images were examined under the fluorescent microscope (Olympus BX60, Center Valley, PA).

Supplementary Material

Refer to Web version on PubMed Central for supplementary material.

Acknowledgments

These studies were supported by NCI MMHCC (National Cancer Institute Mouse Models of Human Cancer Consortium) grant 2U01 CA08422-06 to AB and Program Project Grant (PPG) 5P01AR050440 from the US NIAMS (National Institute Of Arthritis And Musculoskeletal And Skin Diseases), National Institutes of Health (NIH). AB acknowledges support from the Barbara Bass Bakar Chair of Cancer Genetics.

Abbreviations

BCC	basal cell carcinoma
DMBA	dimethylbenzanthracene
K5	keratin 5
K14	keratin 14
NBCCS	nevoid basal cell carcinoma syndrome
SCC	squamous cell carcinoma
SHH	sonic hedgehog
SpCC	spindle cell carcinoma
TPA	12-*O*-tetradecanoylphorbol-13-acetate

References

Aszterbaum M, Epstein J, Oro A, et al. Ultraviolet and ionizing radiation enhance the growth of BCCs and trichoblastomas in patched heterozygous knockout mice. Nat Med. 1999; 5:1285–91. [PubMed: 10545995]

Balmain A, Ramsde M, Bowden GT, et al. Activation of the mouse cellular Harvey-ras gene in chemically induced benign skin papillomas. Nature. 1984; 307:658–60. [PubMed: 6694757]

Barnes EA, Kong M, Ollendorff V, et al. Patched1 interacts with cyclin B1 to regulate cell cycle progression. EMBO J. 2001; 20:2214–23. [PubMed: 11331587]

Burns PA, Kemp CJ, Gannon JV, et al. Loss of heterozygosity and mutational alterations of the p53 gene in skin tumours of interspecific hybrid mice. Oncogene. 1991; 6:2363–69. [PubMed: 1766680]

Byrne C, Tainsky M, Fuchs E, et al. Programming gene expression in developing epidermis. Development. 1994; 120:2369–83. [PubMed: 7525178]

Canamasas I, Debes A, Natali PG, et al. Understanding human cancer using Drosophila: Tid47, a cytosolic product of the DnaJ-like tumor suppressor gene l2Tid, is a novel molecular partner of patched related to skin cancer. J Biol Chem. 2003; 278:30952–60. [PubMed: 12783860]

Chen Y, Struhl G. Dual roles for patched in sequestering and transducing Hedgehog. Cell. 1996; 87:553–63. [PubMed: 8898207]

Chiang C, Litingtung Y, Lee E, et al. Cyclopia and defective axial patterning in mice lacking Sonic hedgehog gene function. Nature. 1996; 383:407–13. [PubMed: 8837770]

Chiang C, Litingtung Y, Harris MP, et al. Manifestation of the limb prepattern: limb development in the absence of sonic hedgehog function. Dev Biol. 2001; 236:421–35. [PubMed: 11476582]

Author Manuscript Author Manuscript Author Manuscript Author Manuscript

Dahmane N, Lee J, Robins P, et al. Activation of the transcription factor Gli1 and the Sonic hedgehog signalling pathway in skin tumours. Nature. 1997; 389:876–81. [PubMed: 9349822]

Davidson EH. Emerging properties of animal gene regulatory networks. Nature. 2010; 468:911–20. [PubMed: 21164479]

Goodrich LV, Milenković L, Higgins KM, et al. Altered neural cell fates and medulloblastoma in mouse patched mutants. Science. 1997; 277:1109–13. [PubMed: 9262482]

Hahn H, Wicking C, Zaphiropoulous PG, et al. Mutations of the human homolog of Drosophila patched in the nevoid basal cell carcinoma syndrome. Cell. 1996; 85:841–51. [PubMed: 8681379]

Hahn H, Wojnowski L, Zimmer AM, et al. Rhabdomyosarcomas and radiation hypersensitivity in a mouse model of Gorlin syndrome. Nat Med. 1998; 4:619–22. [PubMed: 9585239]

Ingham PW, Taylor AM, Nakano Y. Role of the Drosophila patched gene in positional signalling. Nature. 1991; 353:184–87. [PubMed: 1653906]

Johnson RL, Rothman AL, Xie J, et al. Human homolog of patched, a candidate gene for the basal cell nevus syndrome. Science. 1996; 272:1668–71. [PubMed: 8658145]

Kobielak K, Stokes N, de la Cruz J, et al. Loss of a quiescent niche but not follicle stem cells in the absence of bone morphogenetic protein signaling. Proc Natl Acad Sci USA. 2007; 104:10063–8. [PubMed: 17553962]

Kopan R, Fuchs E. A new look into an old problem: keratins as tools to investigate determination, morphogenesis, and differentiation in skin. Genes Dev. 1989; 3:1–15. [PubMed: 2468556]

Lee CS, Buttitta L, Fan CM. Evidence that the WNT-inducible growth arrest-specific gene 1 encodes an antagonist of sonic hedgehog signaling in the somite. Proc Natl Acad Sci USA. 2001a; 98:11347–52. [PubMed: 11572986]

Lee CS, May NR, Fan CM. Transdifferentiation of the ventral retinal pigmented epithelium to neural retina in the growth arrest specific gene 1 mutant. Dev Biol. 2001b; 236:17–29. [PubMed: 11456441]

Li XJ, Du ZW, Zarnowska ED, et al. Specification of motoneurons from human embryonic stem cells. Nat Biotechnol. 2005; 23:215–21. [PubMed: 15685164]

Malanchi I, Peinado H, Kassen D, et al. Cutaneous cancer stem cell maintenance is dependent on beta-catenin signalling. Nature. 2008; 452:650–53. [PubMed: 18385740]

Marigo V, Davey RA, Zuo Y, et al. Biochemical evidence that patched is the Hedgehog receptor. Nature. 1996; 384:176–79. [PubMed: 8906794]

Nagase H, Mao JH, Balmain A. Allele-specific H-ras mutations and genetic alterations at tumor susceptibility loci in skin carcinomas from interspecific hybrid mice. Cancer Res. 2003; 63:4849–53. [PubMed: 12941805]

Oft M, Akhurst RJ, Balmain A. Metastasis is driven by sequential elevation of H-ras and Smad2 levels. Nat Cell Biol. 2002; 4:487–94. [PubMed: 12105419]

Oro AE, Higgins KM, Hu Z, et al. Basal cell carcinomas in mice overexpressing sonic hedgehog. Science. 1997; 276:817–21. [PubMed: 9115210]

Quigley DA, To MD, Pérez-Losada J, et al. Genetic architecture of mouse skin inflammation and tumour susceptibility. Nature. 2009; 458:505–8. [PubMed: 19136944]

Quintanilla M, Brown K, Ramsden M, et al. Carcinogen-specific mutation and amplification of Ha-ras during mouse skin carcinogenesis. Nature. 1986; 322:78–80. [PubMed: 3014349]

Scharer CD, McCabe CD, Ali-Seyed M, et al. Genome-wide promoter analysis of the SOX4 transcriptional network in prostate cancer cells. Cancer Res. 2009; 69:709–17. [PubMed: 19147588]

Seppala M, Depew MJ, Martinelli DC, et al. Gas1 is a modifier for holoprosencephaly and genetically interacts with sonic hedgehog. J Clin Invest. 2007; 117:1575–84. [PubMed: 17525797]

Takahashi K, Yamanaka S. Induction of pluripotent stem cells from mouse embryonic and adult fibroblast cultures by defined factors. Cell. 2006; 126:663–76. [PubMed: 16904174]

Wakabayashi Y, Mao JH, Brown K, et al. Promotion of H-ras-induced squamous carcinomas by a polymorphic variant of the Patched gene in FVB mice. Nature. 2007; 445:761–65. [PubMed: 17230190]

Author Manuscript Author Manuscript Author Manuscript Author Manuscript

Zhang XM, Ramalho-Santos M, McMahon AP. Smoothened mutants reveal redundant roles for Shh and Ihh signaling including regulation of L/R asymmetry by the mouse node. Cell. 2001; 106:781–92. [PubMed: 11517919]

Author Manuscript Author Manuscript Author Manuscript Author Manuscript

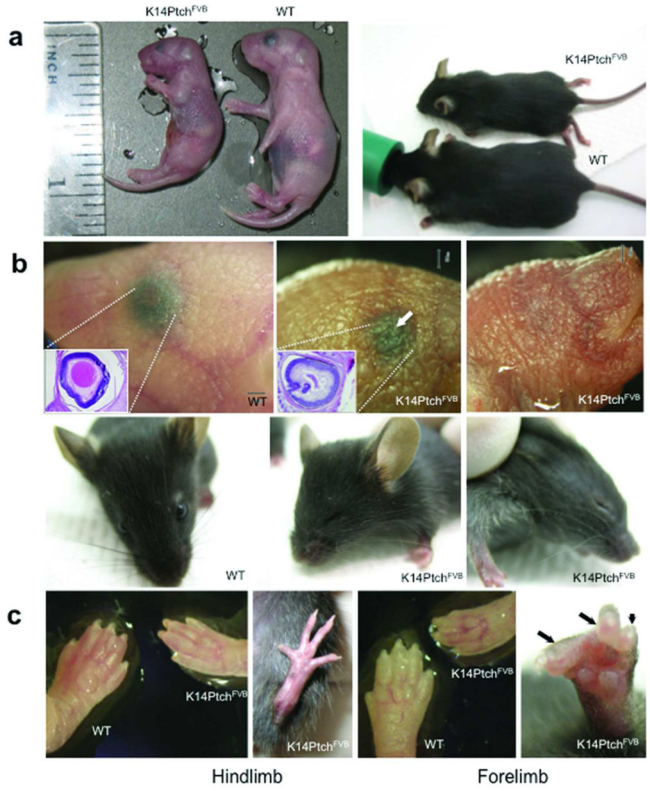

Figure 1. Developmental abnormalities of line 6 *K14Ptch^{FVB}* mice

(a) Gross body size difference between *K14Ptch^{FVB}* and wild-type newborn (left panel) and adult (right panel) mice. **(b)** Ocular developmental defect in line 6 *K14Ptch^{FVB}* mice. Newborn wild-type mice (upper left panel) display normal ocular development with peripheral iris pigmentation and central pupil formation; newborn *K14Ptch^{FVB}* mice (upper center and right panels) either lack pupil formation (arrow) or display hypoplastic ocular development. Adult *K14Ptch^{FVB}* mice exhibit permanently closed eyes (lower center and right panels). **(c)** Abnormal limb development in line 6 *K14Ptch^{FVB}* mice. Wild-type mice have 5 digit hindlimbs and 4 digit forelimbs while *K14Ptch^{FVB}* mice have 4 digit hindlimbs and 3 digit forelimbs.

Author Manuscript Author Manuscript Author Manuscript Author Manuscript

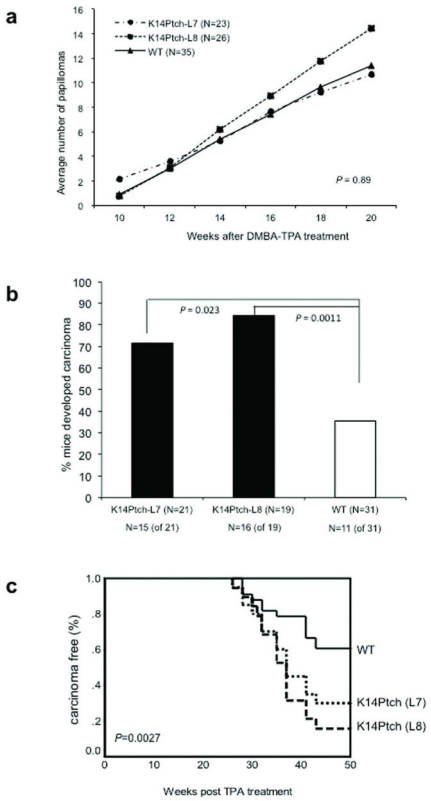

Figure 2. Two-stage skin carcinogenesis in lines 7 and 8 *K14Ptch^{FVB}* and wild-type mice

(L7 for line 7; L8 for line 8). **(a)** Papilloma development in *K14Ptch^{FVB}* and wild-type mice after DMBA/TPA treatment. Average number of papillomas per mouse is comparable between *K14Ptch^{FVB}* and wild-type mice at 20 weeks (P=0.89, Kruskal-Wallis test). **(b)** Carcinoma incidence in *K14Ptch^{FVB}* and wild-type mice. By 50 weeks post-treatment, higher percentage of lines 7 and L8 *K14Ptch^{FVB}* mice develop skin carcinomas than wild-type mice (P=0.023 for line 7; P=0.0011 for line 8; Fisher's exact test). **(c)** Carcinoma-free survival in *K14Ptch^{FVB}* (two lines, L7 and L8) and wild-type mice (P=0.0027, Kaplan-Meier method).

Author Manuscript Author Manuscript Author Manuscript Author Manuscript

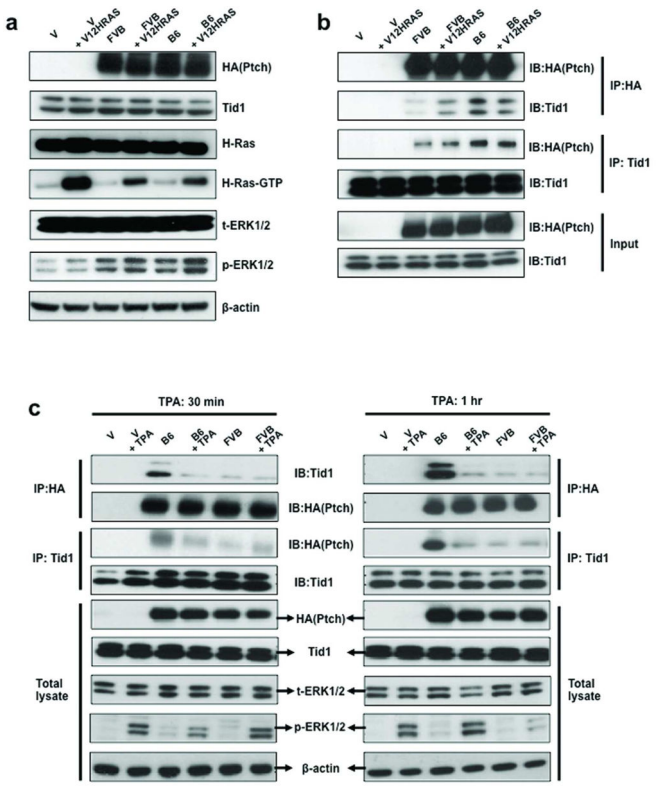

Figure 3. Effect of oncogenic H-Ras and TPA treatment in cells overexpressing *Ptch*^{FVB} or *Ptch*^{B6}

(a) 293T cells were transiently co-transfected with HA-tagged Ptch^{FVB} or Ptch^{B6} and oncogenic V12*HRAS*. MAPK signaling was examined by Western blotting. Co-transfection of *Ptch1* (*Ptch*^{FVB} or *Ptch*^{B6}) in this assay led to only a modest but reproducible stimulation of P-Erk, and this was increased slightly in the presence of oncogenic V12*HRAS*. **(b)** Oncogenic V12*HRAS* had little effect on the differential binding of Tid1 to Ptch^{FVB} or Ptch^{B6} by immunoprecipitation (IP) with anti-Tid1 and anti-HA antibodies **(c)** IP showed that TPA treatment which had a very strong effect on the activation of P-Erk destabilized the strong binding between Tid1 and Ptch1, especially for the Ptch^{B6} variant

Author Manuscript Author Manuscript Author Manuscript Author Manuscript

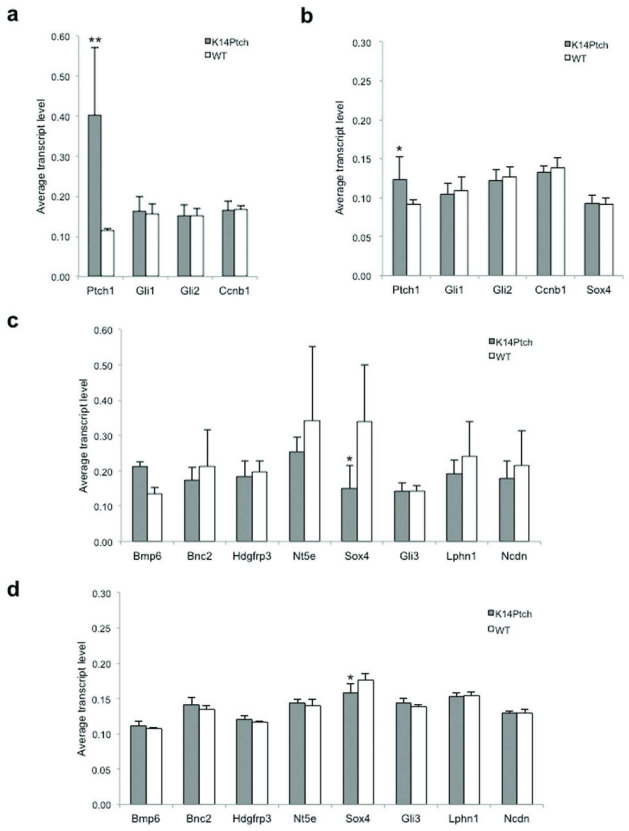

Figure 4. qRT-PCR analysis of the candidate SHH signaling targets

(a) *Ptch1, Gli1, Gli2, and Ccnb1* transcript levels in skins from *K14Ptch*^{FVB} (n=14) and wild-type (n=6) mice. *Ptch1* expression is significantly elevated in the skins of *K14Ptch*^{FVB} mice (P<0.0001 by t-test) **(b)** Average *Ptch1, Gli1, Gli2, Ccnb1, and Sox4* transcript levels in skin cancers from *K14Ptch*^{FVB} and wild-type mice. *Ptch1* expression is also elevated in skin carcinomas from *K14Ptch*^{FVB} mice (P=0.0014 by t-test). **(c)** Analysis of *Bmp6*, *Bnc2*, *Hdgfrp3*, *Nt5e*, *Sox4*, *Gli3*, *Lphn1*, and *Ncdn* transcript levels in adult skins from *K14Ptch*^{FVB} and wild-type mice. The average *Sox4* transcript level is significantly decreased in adult skins of *K14Ptch*^{FVB} mice (P=0.001 by t-test) **(d)** Average *Bmp6, Bnc2, Hdgfrp3, Nt5e, Sox4, Gli3, Lphn1*, and *Ncdn* transcript levels in newborn skins from *K14Ptch*^{FVB} (n=5) and wild-type (n=5) mice. The average *Sox4* transcript level is also slightly lower in newborn skins of *K14Ptch*^{FVB} mice (P=0.023 by t-test). Statistical significance is indicated by * symbol (** for P <0.001; * for P <0.05 by t-test)

Author Manuscript Author Manuscript Author Manuscript Author Manuscript

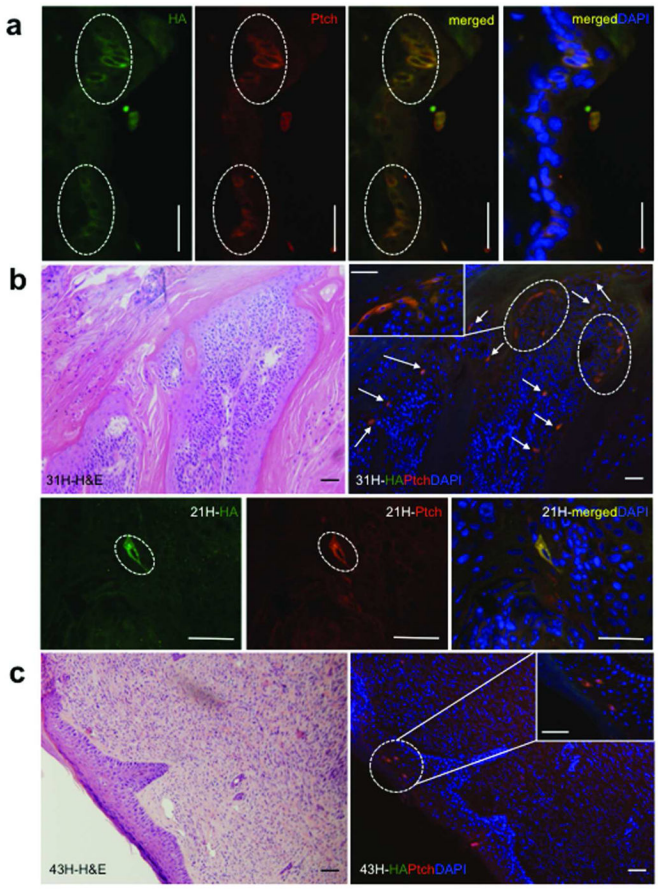

Figure 5. HA/Ptch-positive cells in the normal skin and skin carcinomas of *K14Ptch*^{FVB} mice

(a) HA/Ptch-positive cells (dotted circles) in normal skin from line 6 *K14Ptch*^{FVB} mice by immunohistochemical analysis. **(b)** HA/Ptch-positive cells (arrows and dotted circles) in SCCs from lines 7 and 8 *K14Ptch*^{FVB} mice by immunohistochemical analysis. In the SCCs, the HA/Ptch positive cells were often located at the superficial aspect of the spinous layer, near the interface with the keratinized/cornified cells. Parallel H&E-stained section (upper left panel) reveals well-differentiated SCC. **(c)** HA/Ptch-positive cells (dotted circle and embedded image with higher magnification) are present in the squamous epithelium adjacent to a spindle cell carcinoma. No HA/Ptch staining is seen in the spindled carcinoma cells. Scale bar = 50μm

Author Manuscript Author Manuscript Author Manuscript Author Manuscript

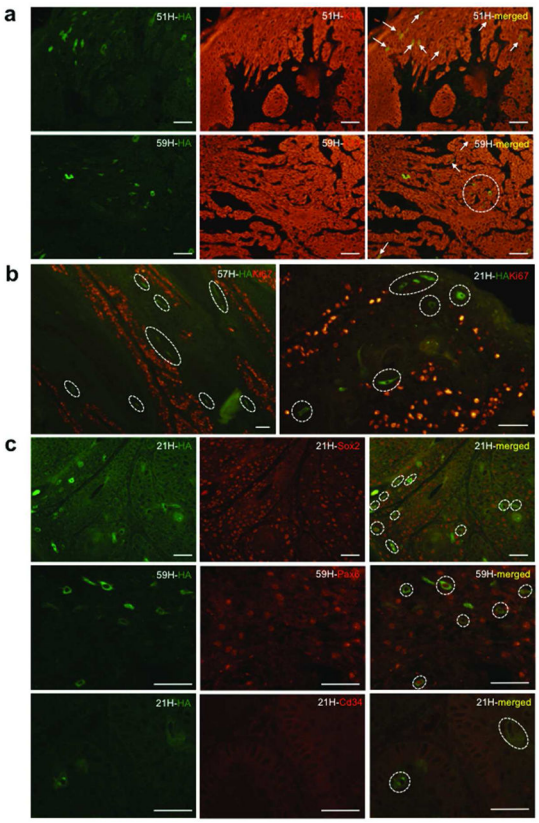

Figure 6. Co-staining of the HA/Ptch-positive cells with K14, Ki67, or stem cell markers in SCCs from *K14Ptch*^{FVB} mice

Arrows and dotted circles indicate HA/Ptch-positive cells. **(a)** Co-staining of HA and K14-positive cells. The HA/Ptch-positive cells are located in SCCs with strong keratin 14 expression. **(b)** Co-staining of HA and Ki67-positive cells. The HA-positive cells (dotted circles) are negative for Ki67 expression. **(c)** Co-staining of HA with stem cell markers, Sox2, Pax6, or Cd34 antibodies. Scale bar = 50μm